IEEE Access
Multidisciplinary | Rapid Review | Open Access Journal

Received August 28, 2018, accepted September 22, 2018, date of publication October 1, 2018,
date of current version November 30, 2018.

Digital Object Identifier 10.1109/ACCESS.2018.2873062

Mutual Coupling Reduction and Pattern Error Correction in a 5G Beamforming Linear Array Using CSRR

RAGHURAMAN SELVARAJU[1], MOHD HAIZAL JAMALUDDIN[1], (Member, IEEE), MUHAMMAD RAMLEE KAMARUDIN[2], (Senior Member, IEEE), JAMAL NASIR[3], AND MUHAMMAD HASHIM DAHRI[1]

[1]Wireless Communication Centre, School of Electrical Engineering, Universiti Teknologi Malaysia, Johor 81310, Malaysia
[2]Centre for Electronic Warfare, Information and Cyber, Cranfield Defence and Security, Cranfield University, Defence Academy of the United Kingdom, Shrivenham SN6 8LA, U.K.
[3]Department of Electrical Engineering, COMSATS Institute of Information Technology, Islamabad 45550, Pakistan

Corresponding authors: Muhammad Ramlee Kamarudin (ramlee.kamarudin@cranfield.ac.uk) and Mohd Haizal Jamaluddin (haizal@fke.utm.my)

This work was supported in part by the Ministry of Education Malaysia, Ministry of Science Technology and Innovation, and in part by the Universiti Teknologi Malaysia under Grant 4J211, Grant 03G59, Grant 4S134, and Grant 19H56.

ABSTRACT A four-element printed antenna array operating at 25-GHz frequency with complementary split ring resonator (CSRR) has been proposed for beamforming applications. The CSRR elements have been used to suppress the mutual coupling in the proposed array. The existence of the CSRR configuration in antenna array controls the unnecessary surface current flow between the array elements, and thus the mutual coupling between array elements has been significantly reduced up to −55 dB. The effect of mutual coupling on the array radiation patterns has been studied in the presence and absence of CSRRs. The effectiveness of the CSRR has been studied by steering the main beam as well as the nulls in different angles. By implementing the CSRR elements in array antenna, the distorted array patterns have been recovered and are presented. The proposed antenna array with the CSRR has the advantage of easy and low-cost fabrication and it offers excellent coupling suppression without changing the antenna profile. The commercially available simulation tools such as MATLAB and Ansys HFSS have been used for array weights calculation and antenna design respectively. Finally, the fabricated prototype has been experimentally verified, and it shows that the analytical and computed results agree well with the measured results.

INDEX TERMS Linear array, beamforming, mutual coupling, nulls, complementary split ring resonator, 5G.

I. INTRODUCTION

Historically, due to the expanded wireless-communication services, the telecommunication innovation has acquired phenomenal growth from the first generation (1G) to fifth generation (5G) wireless standard. Consequently, the world wide unique mobile subscriber numbers have exceeded up to 5 billion, and it has been expected to reach 6 billion by 2020 [1]. Moreover, in recent years wireless gadgets and Internet of Things (IoT) devices usage has exponentially increased. As a result of these quick advancement, the demand for mobile data services has increased significantly. Besides, the large number of communication devices usage causes a strong interference between the devices. In order to cope with the increased data rate demand and to address the interference problem, a new wireless standard is required. Particularly, to support the high-speed communication and improve the quality of services, the data rate of forthcoming wireless standard (5G) should be in the range from 100Mbps (Edge rate) to 1Gbps (peak rate), respectively [2], [3].

Basically, wide operating frequency band is needed to obtain such high data rate. In order to achieve the peak data rate (1Gbps) of the 5G, the required frequency bandwidth must be up to several hundred Megahertz or few Gigahertz [4]. However, Ultra High Frequency (UHF) band (300MHz to 3 GHz) which is currently used for mobile

communication is almost saturated due to several applications. Therefore, wide band allocation for future communication at UHF band is unattainable. Apart from UHF spectrum, there are several higher frequency spectrum bands, which have strong potential to meet some of the 5G demands identified until now [5]. Hence, the International Telecommunication Union Radio Communication Standards Sector (ITU-R) has allocated the frequencies above 6 GHz for the upcoming mobile standard (5G) research [6], [7]. Recently, the higher frequencies have gained a substantial attention of the operators, vendors and academic researchers, due to its unique bandwidth characteristics [6]. But, the friis equation asserts that, in the higher frequencies the path loss will be increased due to its small wavelength [8]. Therefore that the high frequency signals can travel only short distances and easily attenuated by the obstacles due to poor penetration.

Several research works prove that, this problem can be mitigated by employing multiple antennas (antenna array) at transmitter and receiver ends [9].The array antennas possess numerous advantages such as, high gain, narrow beam width etc. However, the array antennas contain limited coverage due to narrow beam in both azimuth and elevation plane. Technically, the coverage of the antenna array can be enhanced by utilizing beam forming technique [10]. The beamforming array is a type of antenna, which place the maximum signal radiation in the desired direction and places nulls in the undesired directions. It has been achieved by exciting the array elements with variable phase or variable time delays [11], [12]. The beam forming array can be constructed by using any type of radiating elements. However, printed type (microstrip patch) radiators are highly suitable to construct a compact and lightweight beam forming antenna array. Another interesting advantage of microstrip patch is that its easy integration with beamforming circuits [13]. The aforementioned advantages encouraged the antenna designers to pay greater attention on microstrip patch beam forming antenna arrays.

The mutual coupling alters the individual element patterns as compared to its isolated patterns, causing impedance variation and correlation of the signals. This alteration depends on the position of the element in the array. The individual element parameters like input impedance, radiation pattern etc. al alteration degraded the array performance, which results in the overall system performance degradation [14]–[17]. Various mathematical methods such as, open circuit voltage method [18]–[20], calibration method [21], [22], receive mutual impedance approach [23] and perturbation method [24] have been proposed to compensate the effect of mutual coupling. However, these mitigation methods are well suitable only for small arrays. Because, higher number of elements in an array increases the calculation complexity of these methods. Apart from these compensation methods, recently, materials gained much attention in the field of electromagnetic due to its peculiar characteristics. In general, the materials which have negative characteristics (negative electrical permittivity and / or negative magnetic permeability) are referred as metamaterials [25], [26].

Periodic arrangements of these negative materials do not allow the surface current flow from one antenna element to another, thus the mutual coupling between antenna elements is reduced. Various meta materials configurations such as, high impedance surfaces (HIS) [27], Defected Ground structures (DGS) [28]–[30], Electromagnetic Band Gap structures (EBG) [31], Split Ring Resonator (SRR) [32], [33] and complementary split-ring resonator (CSRR) [34]–[37] have been reported in past studies to enhance the isolation between array radiators. The defected structures which could be located in ground are large in size, therefore they can increase back-radiation. Next, the EBG configurations are complex in design because multi-layer substrate and vertical via's are required to construct these structures. Implementing these EBGs increases the design complexity of beamforming array. Comparatively, the CSRR configurations offer higher mutual coupling reduction than others. In general, the CSRR is a negative permittivity artificial material and it is a negative image of SRR. It has been obtained by replacing the SRR metal parts with apertures, and the apertures with metal plates [38]. The inspiration for the SRR structure, and its counterpart (CSRR), comes from babinets principle in diffraction theory, which in its general form relates the relation of one particular screen with its complementary [39], [40]. Furthermore, these structures are compact in size, simple in design and easy to integrate with the antenna arrays.

In [36] a slot combined CSRR filtering structure has been used to decouple the two element antenna array. To reduce the coupling between antenna elements, three SCSRRs are etched in the ground plan. The SCSRRs block the surface current flow from one antenna element to other. Therefore, an 10 dB coupling reduction has been achieved. Next, in [35] a ring shape CSRR has been used to decouple the four-element printed MIMO antenna. The CSRR elements have been etched on the common ground plan of the MIMO antenna. The presence of CSRR's controls the surface current flow from one antenna to another. Thus, the mutual coupling of -10 dB has been obtained between closely ($0.17\,\lambda$) placed MIMO antennas.

Several research works propose different CSRR configurations for mutual coupling reduction. However, those CSRR elements are only used to decouple simple array antennas. Only few research works investigate the performance of the CSRR configurations along with beamforming antenna arrays. Hence, in this research work the CSRR configuration is chosen to decrease the mutual coupling between beamforming antenna array and the radiation performance of the beamforming antenna array has been verified along with CSRR elements when the main beam and nulls are steered to different angles. By doing so it will be justified that CSRRs not only suppress mutual coupling when the main beam is pointing in the broadside direction (as discussed in most studies) but are also effective when the main beam is scanned off broadside direction.

In accordance to the above discussion, the development of a beam-forming antenna array with high gain and less mutual coupling is most essential for future wireless (5G) system. In order to address these issues, this research work focuses on two major aspects; beamforming microstrip patch array and reduction in mutual coupling in beam forming array using CSRR. Design of beamforming microstrip patch antenna array is discussed in section II, next the design of complementary split ring resonator is presented is section III. Followed by mutual coupling reduction and the radiation performance enhancement on the beamforming array using CSRR is elaborated in section IV. Finally, in section V, the experimental results are explained in detail.

II. FOUR-ELEMENT MICROSTRIP PATCH ANTENNA ARRAY

Consider a four-element MPA array along the y-axis as shown in Fig. 1. The dimensions of the proposed antenna have been calculated using transmission line model [10]. The optimized dimensions are listed in Table 1. The standard duroid material with $\varepsilon_r = 2.2$ and 0.254 mm thickness is used as substrate material. As displayed in Fig. 1, microstrip antennas are placed side by side to form a four-linear array. The center to center element spacing (S) have been maintained as 8 mm, which corresponds to the wavelength of 0.67 λ at 25 GHz. The computed and experimental S-parameters results of the configured linear array (reflection and transmission coefficients) is presented in Fig. 2. The results clearly show that, all four radiators are operating at 25 GHz, while the strongest mutual coupling is recorded between the element 1 & 2(S_{12}), which is close to −23.2 dB.

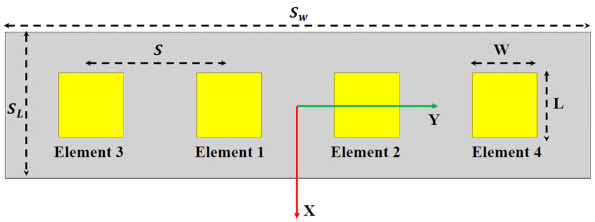

FIGURE 1. Four elements linear array.

TABLE 1. Microstrip patch design parameters.

Parameter	Value (mm)	Parameter	Value (mm)
S_L	32	L	3.76
S_W	8.6	W	3.76
h	0.254	Q	0.6

The array factor of a uniformly placed linear array with an four identical elements that are arranged along the y-axis, is given by [14]:

$$AF = W_{-2}e^{-j\left(\frac{3}{2}\right)\Psi_{-2}} + W_{-1}e^{-j\left(\frac{1}{2}\right)\Psi_{-1}} + W_1 e^{j\left(\frac{1}{2}\right)\Psi_1} + W_2 e^{j\left(\frac{3}{2}\right)\Psi_2} \quad (1)$$

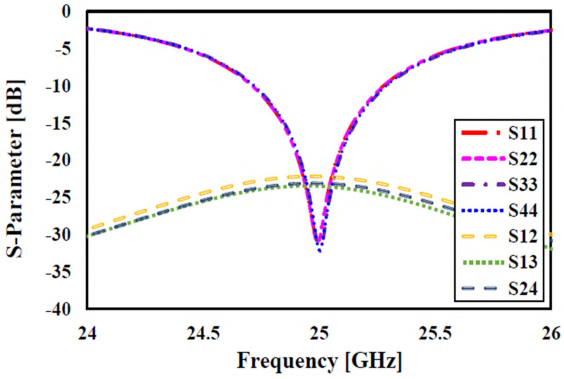

FIGURE 2. S- parameters of the proposed linear array.

and

$$\Psi_n = \frac{\pi\,(n)\,S}{\lambda}\sin(\theta), \quad n = \pm 1, \pm 2. \quad (2)$$

Where W_n is the excitation coefficient (the complex array element weights), which is the determinant factor of the linear array radiation pattern. The angle θ represents the direction of the targeted main beam and null direction. In this work, three beamforming radiation patterns have been defined for different values of θ. The targeted main beam and nulls directions for all three patterns are summarized in Table 2.

TABLE 2. Summary of beamforming patterns.

Pattern	Scan angle θ_U	Null 1 θ_{N1}	Null 1 θ_{N2}	Null 1 θ_{N3}
1	0°	-25°	$+25^\circ$	$+50^\circ$
2	$+15^\circ$	-35°	-10°	$+40^\circ$
3	$+20^\circ$	-04°	-35°	-60°

In order to drive the array main lobe at θ_U and three nulls at θ_{N1}, θ_{N2} and θ_{N3} the complex array elements weights $(W_n's)$ are required. The complex weights are computed through linear algebra method and it is given by [10]:

$$W_n = A^{-1}y \quad (3)$$

where

$$A = \left[\bar{a}_1\ \bar{a}_2\ \bar{a}_3\ \bar{a}_4\right]$$

and

$$\bar{a}_n = \left[e^{-j\left(\frac{1}{2}\right)\Psi_{-1}}\ e^{-j\left(\frac{3}{2}\right)\Psi_{-2}}\ e^{j\left(\frac{1}{2}\right)\Psi_1}\ e^{j\left(\frac{3}{2}\right)\Psi_2}\right]$$
$$y = \left[1\ 0\ 0\ 0\right]$$

Where y is a 4×1 forcing function matrix for the steering vector matrix A. Finally, the complex ideal array element weights computed using Equation 3 for the desired scan angles (as in Table 2) has been presented in Table 3. It contains the input weights in power and phase form. Furthermore, these weights are calculated under ideal conditions without considering the effects of mutual coupling.

The calculated complex weights have been fed into the HFSS simulation tool. As pointed out previously, the weights

TABLE 3. Array elements complex weights.

	Port 1		Port 2		Port 3		Port 4	
Pattern	Power (dBm)	Phase (deg)	Power (dBm)	Phase (deg)	Power (dBm)	Phase (deg)	Power (dBm)	Phase (deg)
1	−7	0	−7	0	−10	2	−10	−2
2	−7	32	−7	−32	−9	77	−9	−77
3	−8	52	−8	−52	−6	89	−6	−89

are calculated without considering the effects of mutual coupling. However, in simulation the mutual coupling effect has been taken into account. Therefore, the simulated array radiation patterns are distorted from the ideal array pattern that is calculated by using Equation 1. For further clarification on the ideal and simulated beamforming patterns of the four-element linear array is presented in Fig. 3.

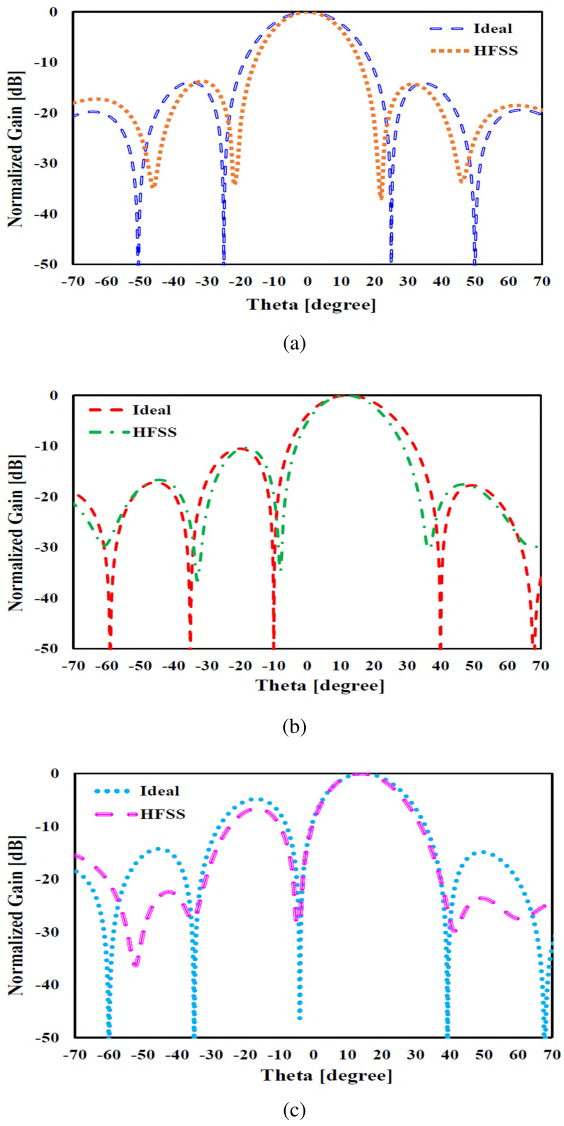

FIGURE 3. Beamforming radiation pattern. (a) Pattern 1. (b) Pattern 2. (c) Pattern 3.

By examining the results, the main beam positions of the ideal and simulation radiation patterns are almost matched in all three beamforming patterns. However, in simulated beam patterns, the nulls positions and the depth are considerably differed as compared to the ideal array pattern. Furthermore, the beamwidth of the simulated patterns are also slightly reduced. This reduction and shifting in the nulls depth and position is because of the effect of mutual coupling. The solution to this problem is to reduce the mutual coupling between the antenna array elements. In order to reduce the mutual coupling between the array elements, a complementary split ring resonator (CSRR) has been proposed in this work. Therefore in next section the design and analysis procedure of the CSRR element is explained in detail.

III. COMPLEMENTARY SPLIT RING RESONATOR

The mathematical analysis for SRR and its dual counterpart structure CSRR is identical with a suitable interchange of electric and magnetic quantities. In order to achieve the design goal, the dimensions of negative permittivity SRR has initially been calculated and designed. Later, by applying the duality principle the configured SRR structure has been transformed into complementary structure by replacing the conductors part as aperture. The band rejection frequency of the SRR has been numerically calculated using Equation 4. Basically, the total inductance (L) and capacitance (C) of the SRR model are related to the dimensions of the SRR. The relation between the SRR dimensions and resonance frequency has been extensively explained in [37] and [41].

$$f_0 = \frac{1}{2\pi\sqrt{LC}} \tag{4}$$

In order to numerically characterize the SRR inclusions, the proposed unit cell is designed and positioned at the center of the air-filled waveguide, as shown in Fig. 4. In simulation, the top and bottom sides of a waveguide boundary box are defined as PMC, while its side walls are attributed as PEC walls and the front and back are used for the signal excitation. The computed scattering parameters (S_{11} and S_{12}) of the configured SRR, are shown in Fig.5a. The proposed filtering elements exhibit a sharp band rejection at 25 GHz.

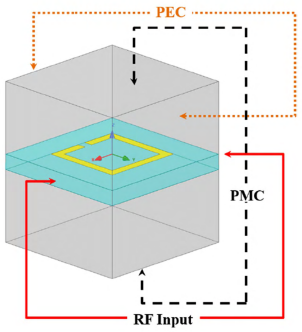

FIGURE 4. Unit cell simulation setup.

Moreover, the permittivity (ε) and permeability (μ) of the proposed structure are calculated from the scattering (S)

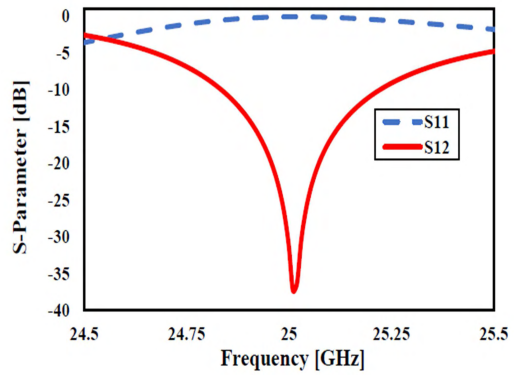

(a)

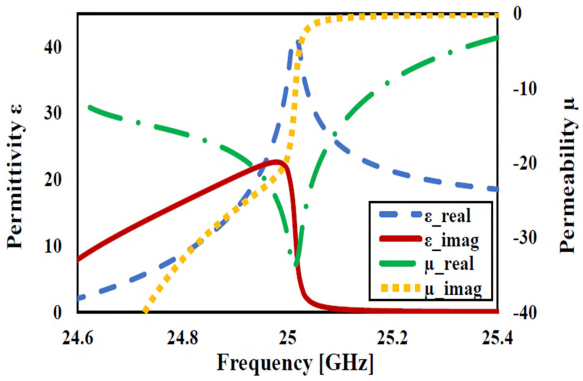

(b)

FIGURE 5. Simulated results of SRR unit cell. (a) Scattering parameter response. (b) Constitutive properties.

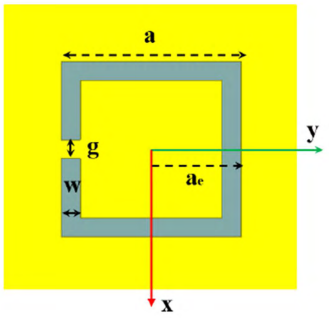

FIGURE 6. CSRR unit cell.

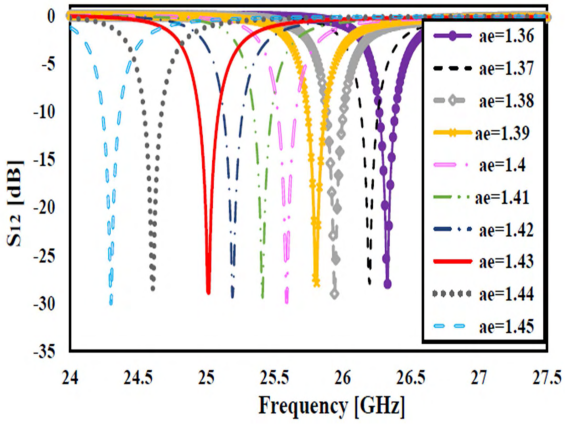

FIGURE 7. S_{12} for different values of 'a'.

parameters as given by the following Equation 5 [42], [43].

$$\varepsilon = \frac{n}{z}; \quad \mu = n \times z \tag{5}$$

Where refractive index (n) and the wave impedance (z) are calculated using the following equations [42], [43].

$$n = \frac{1}{kd}\cos^{-1}\left[\frac{(1 - S_{11}^2 + S_{21}^2)}{2S_{21}}\right] \tag{6}$$

$$z = \sqrt{\frac{(1 + S_{11})^2 - S_{21}^2}{(1 - S_{11})^2 - S_{21}^2}} \tag{7}$$

The calculated constitutive properties are presented in Fig. 5b, the results clearly show the negative responses of permeability that can be obtained by configured SRR.

In order to obtain the negative permittivity filtering structure, the configured SRR structure has been transformed in to complementary structures using the concept of dual electromagnetic behavior. The configured complementary SRR filtering element is shown in Fig 6. The band stop response of the CSRR structures is slightly varied as compared to the SRR configuration. In order to obtain the stop band response at 25 GHz, the dimensions of the CSRR configuration has been optimized. The computed scattering parameters of the CSRR model for different values of a are displayed in Fig. 7.

The parametric results clearly shows that, the stop band response at 25 GHz is observed at $a = 1.43$ mm. The optimized dimensions of the modeled CSRR configuration are listed in the Table 4.

TABLE 4. CSRR unicell dimensions.

Parameters	Value (mm)
a	1.43
w	0.15
g	0.15
t	0.035

The S-parameter and constitutive properties of the optimized CSRR element are given in Fig. 8. The simulation results prove that, the configured complementary structure offer band rejection at 25 GHz and the constitutive results clearly shown that, the complementary structure have negative permittivity response at the required 25 GHz. This negative permittivity CSRR filtering element has capability to decouple the electrically coupled radiating elements. Therefore, in next section the CSRR filtering element is implemented in the four-element beamforming linear array and its performance is studied and compared with conventional antenna array.

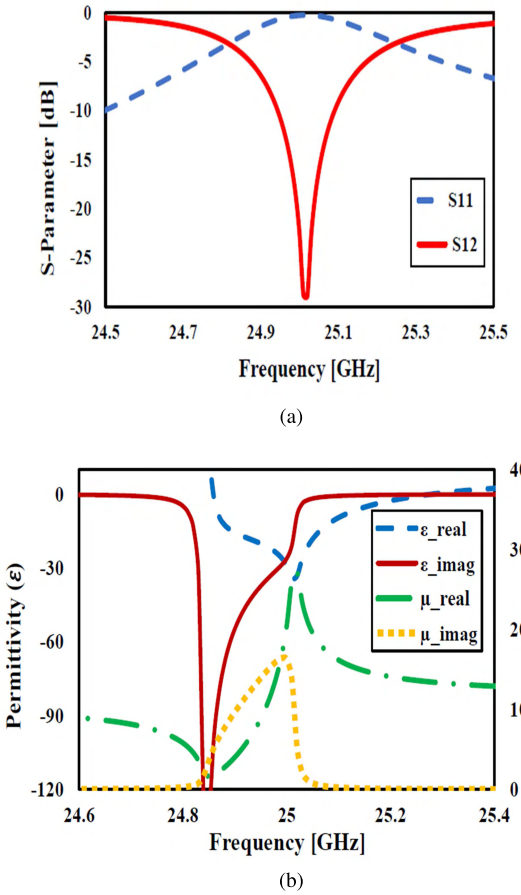

FIGURE 8. Simulated results of CSRR unit cell. (a) Scattering parameter response. (b) Constitutive properties.

IV. MUTUAL COUPLING REDUCTION IN ANTENNA ARRAY USING CSRR

In order to reduce the surface current flow and the mutual coupling between the array radiating elements, an array of CSRR's have been implemented in between radiating element. The CSRR's have been arranged in three different orientations such as; parallel orientation (PO), face to face orientation (FFO) and opposite faced orientation (OFO) as shown in Fig. 9 respectively.

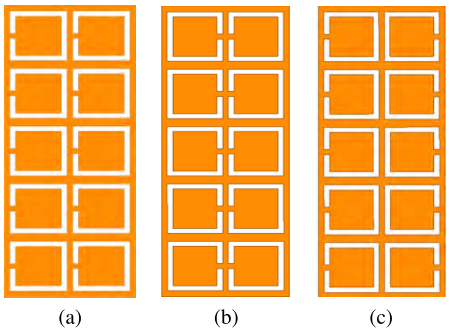

FIGURE 9. Different orientation of CSRR elements. (a) Parallel (PO). (b) Face to face (FFO). (c) Opposite faced (OFO).

Initially, the CSRR elements are implemented in between the radiators on the top surface of the proposed array, later they have been etched in the ground plan, finally the CSRR elements are implemented in both top and ground surface. The filtering capability of all the nine different configurations has been verified in terms of transmission coefficient (S_{12}). The comparison of the simulated transmission coefficient results of all the nine different configurations are presented in Fig. 10. The results clearly show that, as compared to all other configurations the antenna array which contains opposite faced CSRR elements in both top and ground surface have minimum (−44 dB) mutual coupling at the required frequency of 25 GHz.

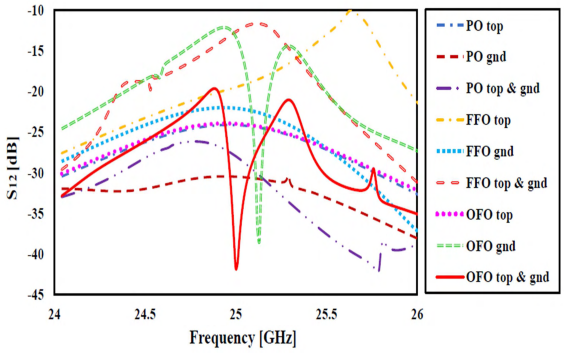

FIGURE 10. Mutual coupling (S_{12}) between antenna array with different CSRR configurations.

Finally, the Four-element linear antenna array with opposite faced CSRR elements in both top and ground configuration, which is shown in Fig. 11, is chosen as final design. Fig. 12 presents the computed scattering parameter responses of the finalized Four-element linear antenna array configuration. As it can be observed from Fig. 12, the mutual coupling between all the array elements are reduced to −44 dB at the operating frequency of 25 GHz. The obtained additional

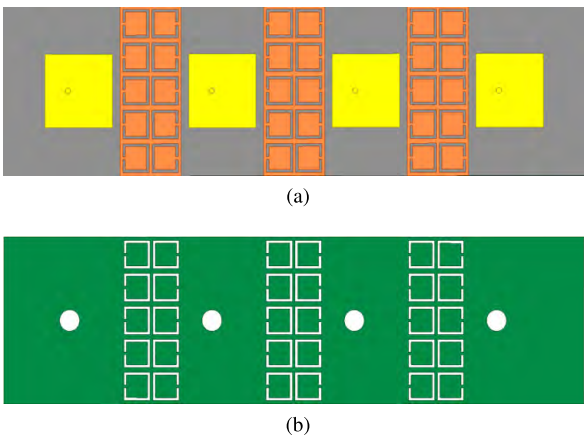

FIGURE 11. Antenna array with opposite faced CSRR elements. (a) Top surface. (b) Ground.

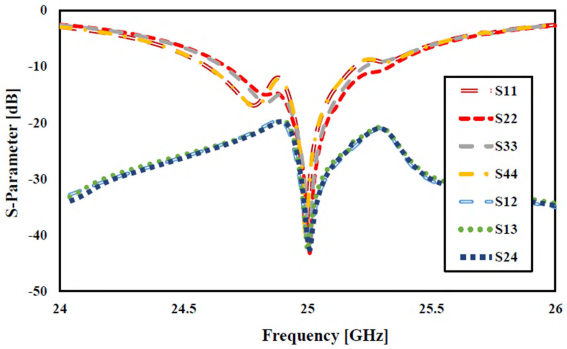

FIGURE 12. S-parameters of the antenna array with opposite faced CSRR.

coupling suppression is nearly 22 dB higher than the simple four-element antenna array (Fig. 2).

Furthermore, for clarification, the surface current distribution of the four-element antenna array with presence and absence of CSRR elements is analyzed when one port is excited while other ports are terminated with 50 Ω impedance. The surface current distribution of the array antenna is presented in Fig. 13. In general the surface current is high in active port and zero at terminated ports. However, by observing the Fig. 13a the surface current is extremely high in active element at the same time small amount of current distribution has been observed in the neighboring elements. In Fig. 13b the surface current flow from the active element to the neighboring elements is controlled by the CSRRs, thus the neighboring elements are completely terminated and almost zero current has been observed.

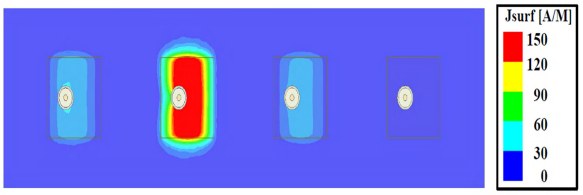

(a)

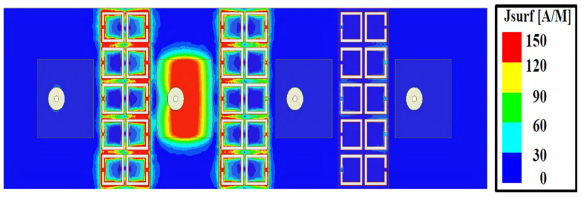

(b)

FIGURE 13. Current distribution in four-element antenna array. (a) Without CSRR. (b) With CSRR.

The aforementioned results confirm that, the presence of the CSRR elements in antenna array control the surface current flow and increase the isolation between array radiators. Hence, the excitation coefficients (which are related to the array radiation) of the array elements are not affected by the mutual coupling.To confirm that, the complex weights given in Table 3 have been fed in to the CSRRs implemented four-element antenna array.

The radiation patterns of the proposed antenna array have been computed and compared with the ideal and simple (without CSRR) antenna array radiation pattern (Fig 14). Fig. 14 shows the CSRR implemented array antennas simulated beam patterns along with the ideal and simple array antenna beam patterns. As compared to the simple array (without CSRR) radiation patterns, the proposed array radiation patterns are very close to the calculated ideal patterns.

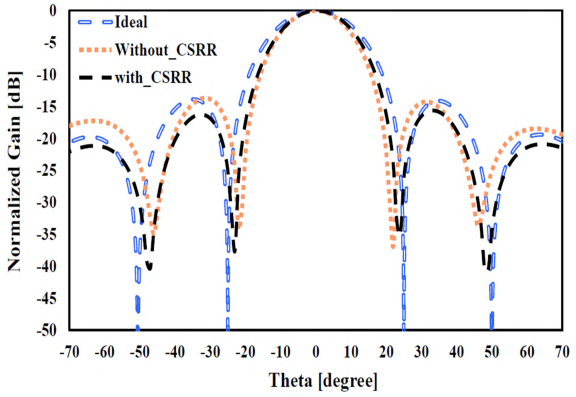

(a)

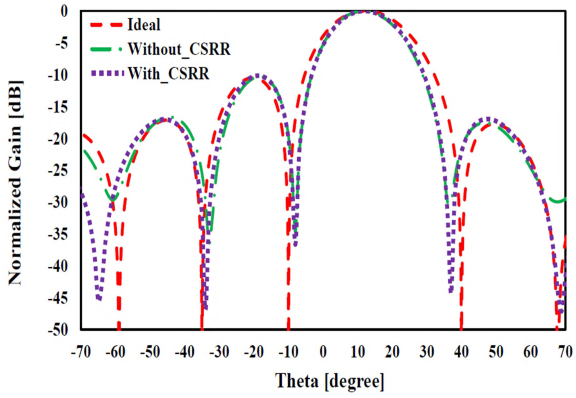

(b)

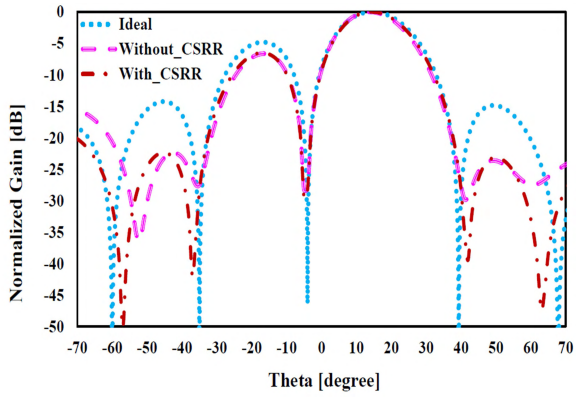

(c)

FIGURE 14. Simulated beamforming radiation pattern comparison of four-element antenna array. (a) Pattern 1. (b) Pattern 2. (c) Pattern 3.

Specifically, the nulls positions in the CSRR implemented array pattern, when the main beam is at 15′(Fig. 14b), have moved to −34′, −9′ and 39′, though the nulls depths are increased up to −45 dB. The nulls in the ideal pattern is located at −35′, −10′ and 40′respectively, with the null depth of $-50dB$. Similarly, the beam pattern of the array when the main beam is at 20′is shown in Fig. 14c. Here, the first null has deepened to about −30 dB and located at the same position of the null in the ideal pattern and other two nulls are located at −36′ and −59′with −45 dB and −50 dB depth respectively. In ideal pattern, the nulls are located at −4′, −35′and −60′, though the depth are very deep. The results depict that, the nulls depth are significantly increased in proposed antenna arrays, also the nulls positions are fairly conjoined with the calculated nulls positions.

V. EXPERIMENTAL RESULTS

To investigate and validate the effects of mutual coupling, a four-element printed antenna array with and without the CSRR elements has been fabricated, as shown in Fig. 15. The array elements are fed by molex flexible cable assemblies. Furthermore, the inner conductor of the cable is adhered to the patch element via a conducting glue and the outer conductor of the cable is soldered to the antenna common ground plane.

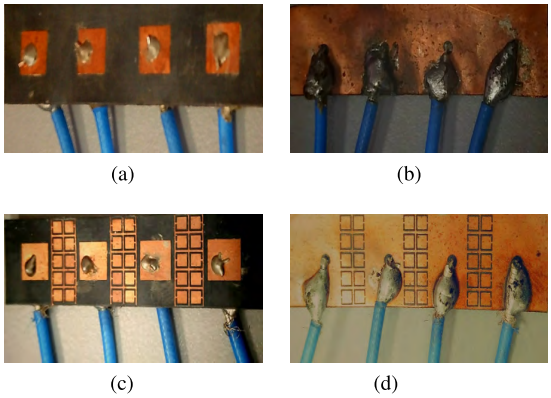

FIGURE 15. Fabricated four-element antenna arrays. (a) Simple array front view. (b) Simple array back view. (c) CSRRs loaded array front view. (c) CSRRs loaded array back view.

A. MEASURED SCATTERING PARAMETER RESULTS

Initially, the scattering parameter measurements for the antenna array have been carried out using keysight PNA-L network analyzer. Before starting the measurement the PNA has been properly calibrated so that the RF cable losses can be properly considered, and their effects are removed from the measurements. Two elements have been measured at a time, while the other two elements have been terminated with matched loads. This has to be done because the PNA has only two ports to measure. The experimental S-parameter results of antenna array with and without CSRR elements are presented in Fig. 16. The experimental results are slightly shifted in both with and without CSRR array antenna case. This shift has been observed due to fabrication inaccuracies and the use of conducting adhesives that has been used to

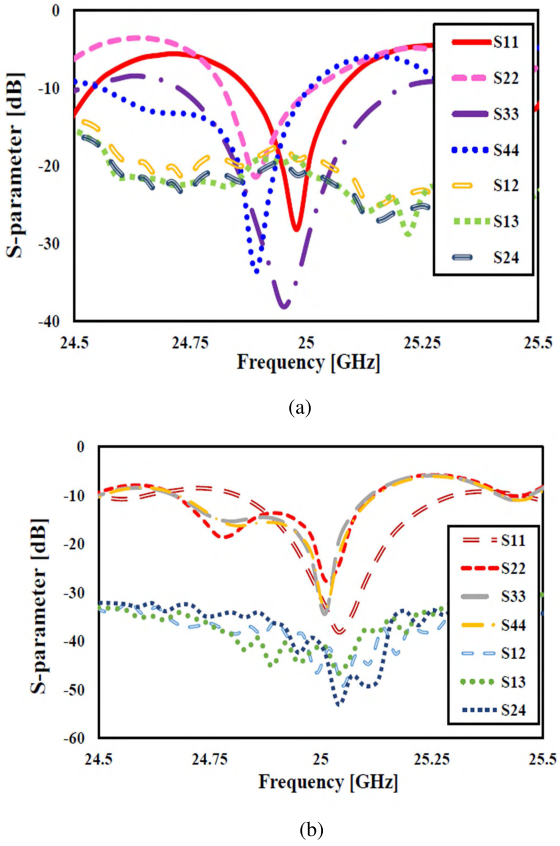

FIGURE 16. Measured S- parameter results of the antenna array. (a) Without CSRR. (c) With CSRR.

attach the antenna elements and co-axial probe. With the help of CSRR's the minimum coupling level of −55 dB has been obtained between the element 2 and element 4. Overall, the computed and experimental S-parameters results of both antennas are in close agreement with minor deviations that has been explained previously.

B. BEAMFORMING MEASUREMENTS

In this section, the four-element antenna array beamforming measurement procedures and the measured beam patterns of the simple and CSRR loaded antenna arrays are described in detail. The measurement setup is presented first that is followed by the measurement results.

1) BEAMFORMING EXPERIMENTAL SETUP

The block diagram of the experimental setup is presented in Fig. 17a. It includes the RF components such as, a low noise amplifier (LNA) ($R18G31GSA$), 4-way power divider (4WPD) ($RFLT4W6G40G$), four voltage variable attenuator (VVA) ($RFVAT0430A30$) and four voltage variable phase shifter (VVP) ($RVPT2229GBC$). As shown in Fig. 17, the LNA feeds the power divider, then four attenuators are attached to the output ports of the power divider. Then four phase shifters are attached to the output ports of each attenuator. Finally the printed antenna array elements are connected to the phase shifters output ports. By varying the

TABLE 5. Performance comparison.

Ref	Approach	Freq [GHz]	Design Complexity	Element Spacing [λ]	Coupling Reduction [dB]	Antenna Radiation Performance Improvement Using Metamaterial	Beamforming Analysis
[30]	DGS	0.97	Low	0.265	10.6	Not specified	Not performed
[31]	EBG	2.50	High	0.50	16	Not specified	Not performed
[32]	SRR	1.24	Moderate	0.125	20	1.4 dB gain improvement	Not performed
[33]	Double negative SRR	28.0	High	Not specified	12	4.3 dB side-lobe reduction	Not performed
[34]	Slot combined CSRR	3.70	Moderate	0.5	19	0.57 dB gain improvement	Not performed
[36]	Slotted CSRR	5.00	Low	0.50	10	No changes in antenna radiation pattern	Not performed
	Proposed CSRR	25.0	Low	0.67	31.8	side-lobe levels are maintained at -20 dB and nulls depth are significantly reduced up to -50 dB	Performed (The main beam of the antenna array is steered to three different angles)

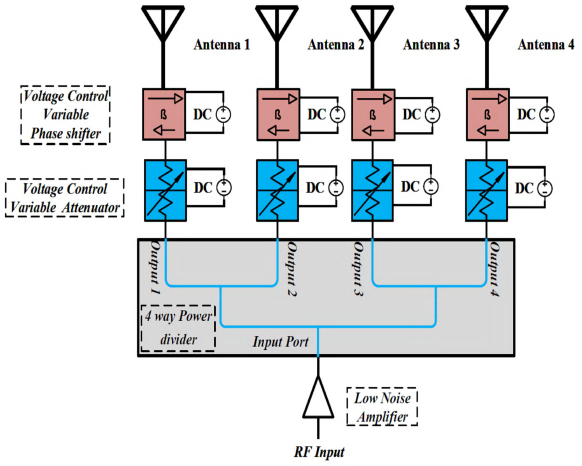

(a)

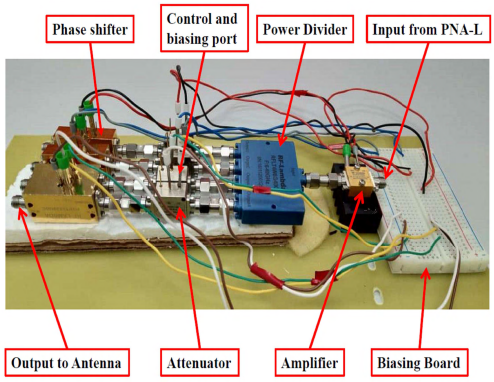

(b)

FIGURE 17. Beamforming measurement setup. (a) Block diagram. (b) Real time setup.

biasing voltage, the VVA and VVP provide different values of attenuation and phase shift. The control voltages were fed by the dual port variable DC power source. The real time controller setup is shown in Fig. 17b.

In order to perform the beamforming measurements, it is necessary to know the output attenuation and phase of the real time controller setup. To evaluate the controller setup, port 1 of the PNA-L is connected to the amplifier, whereas port 2 is connected to the phase shifter output port, as shown in Fig. 18. The biasing voltages of both voltage variable RF-components are fixed to a value that is close to the computed weight. Finally, the transmission coefficient $'S'_{21}$ provides the actual magnitude and phase of the particular output port. The values of those signals should be nearly equal to the calculated weights which are provided in Table 3. This process is repeated for the other ports and other beam scan angles. The particular values of the control voltages for all the attenuators and phase shifters, which give the required attenuation and phase shift for different beam angles, have been noted and later used for antenna array radiation measurements.

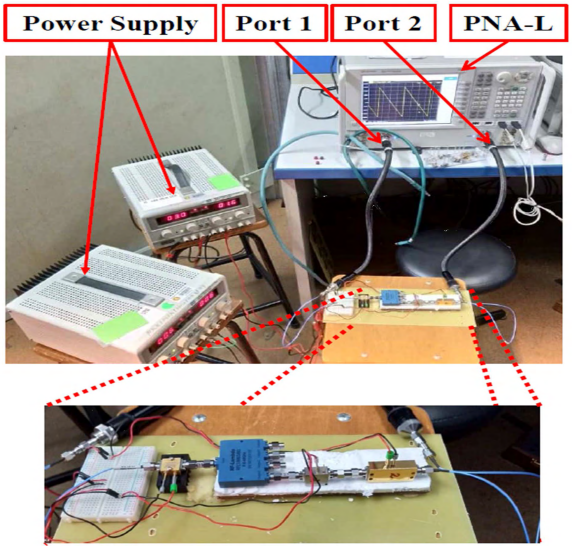

FIGURE 18. Feed network measurement setup.

After getting satisfactory results in the above step, the radiation pattern measurements have been carried out in the NSI anechoic chamber. One port of the PNA-L has been connected to the NSI waveguide probe, which was serving as a receiving antenna. The other port of the PNA-L has been connected to 1×4 equal power divider via LNA to compensate for the cable losses. A power of 2 dBm has been provided from the PNA-L. The outputs of the 4WPD have been connected to the antenna elements via VVA and VVP to achieve the individual weights to be fed to each array element for beamforming applications. Fig. 19 shows the over all beamforming experimental setup in NSI-chamber.

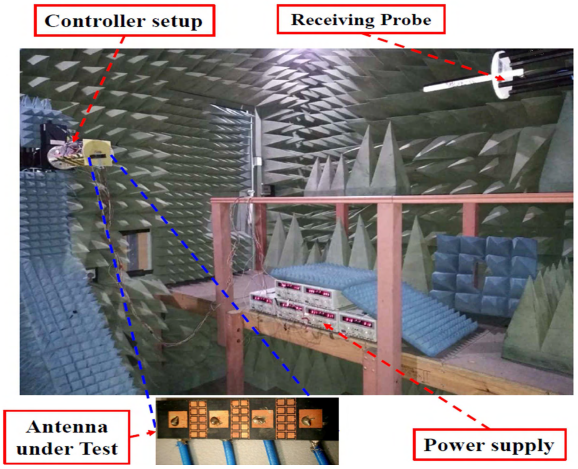

FIGURE 19. Measurement setup in anechoic chamber.

2) MEASURED BEAMFORMING PATTERN RESULTS

The four-element linear antenna arrays, which are displayed in Fig. 15, have been driven with the calculated element weights using VVA and VVP. The beamforming radiation patterns obtained from the experimental setup are shown in Fig. 20. The simple array antenna experimental pattern results are severally affected due to the mutual coupling. However, by observing Fig. 20, it can be easily seen that, the proposed array with CSRR gives better results than the simple antenna array.

All three measured pattern results of the proposed array show that, all the nulls positions are almost matched with the calculated ideal array patterns with the nulls depth of up to -40 to -50 dB. Specifically, the measured beam pattern of the array, when the main beam is at $15'$and the nulls are at $-10'$,$-35'$ and $+40'$ is shown in Fig. 20b. By observing the results, it can be clearly concluded that the nulls position in the simple array pattern are $\pm2-3'$ deviated from the ideal one. At the same time, the nulls in the CSRR implemented array pattern have the same location as the nulls in the ideal pattern. Moreover, the null located at $-10'$is deepened to -30 dB in both simple and proposed array patterns. However, in CSRR implemented array pattern, the other two nulls are deepened about -45 dB, which is nearly 15 dB higher that the simple array patterns nulls depth.

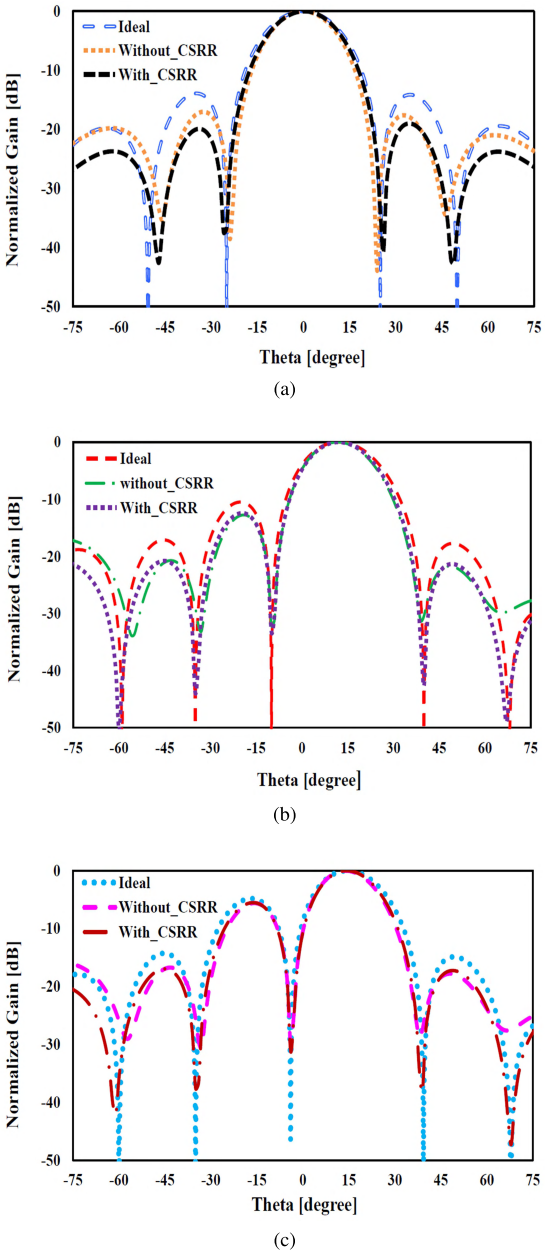

FIGURE 20. Measured beamforming radiation pattern of four-element antenna array. (a) Pattern 1. (b) Pattern 2. (c) Pattern 3.

Similarly, the measured beam pattern when the main beam is pointing towards $20'$, is shown in Fig. 20c. In Fig. 20c the ideal pattern nulls are placed at $-4'$, $-35'$ and $-60'$. By comparing the both antenna array patters with ideal pattern, its clear that the simple array pattern has failed to matched with the calculated ideal array pattern. The first null in the simple array is positioned in same location, but the second and third nulls has moved to $-32.5'$ and $-55'$. In CSRRs implemented array pattern the first two nulls are perfectly placed at $-4'$ and $-35'$, the third null is slightly shifted from the calculated position and located at $-61'$. In addition, all the nulls in the CSRRs implemented array pattern are deeper than the simple array one. The over all results of this work proves that, reducing the mutual coupling between

the array elements using CSRR helps to obtain the optimum beamforming performance that is very close to the ideal ones those are considered free of mutual coupling.

Finally, a comparison between the proposed approach and other metamaterials based techniques is summarized in Table 5. The proposed CSRR filtering element implemented antenna array offers better isolation enhancement than the other metamaterial structures, listed in Table 5.

VI. CONCLUSION

In this article, a four-element microstrip patch antenna array with complementary split ring resonators for mutual coupling reduction was considered for 5G beamforming application. To investigate the radiation characteristics of the proposed array, three beamforming radiation patterns (main beam at 0′, 15′and 20′) have been considered. The Linear Algebra Method has been utilized to calculate the array elements weights those were then used to steer the main beam in a particular direction and place nulls in other undesired directions. Then the effect of the mutual coupling has been analyzed on all three beamforming patterns. The single negative CSRR has been designed and implemented to reduce the coupling between the array radiators. For the real time verification, the prototype of the antenna array with and without CSRR elements has been developed and the performances were validated in terms of scattering parameters and antenna array beamforming patterns. The voltage variable phase shifters and attenuators has been used for practical implementation of those array element weights. The experimental and computed outcomes showed good agreement. It has been concluded from the experimental results that, the mutual coupling between the array elements has been significantly reduced and the array beamforming patterns has been recovered by implementing the complementary split ring resonators in antenna array. And most importantly, to the best of the authors knowledge, it was observed for the first time that the CSRR worked efficiently in reducing the effect of mutual coupling when the beam was steered off broadside. Previously, CSRR or SRR were implemented in arrays with broadside radiation pattern only and almost no study was carried out on on the effectiveness of CSRRs in a smart beamforming array when the main beam as well as position of nulls was changed to different angles.

REFERENCES

[1] "Global mobile trends 2017," GSMA Intell., Tech. Rep., Sep. 2017. Accessed: May 20, 2018. [Online]. Available: https://www.gsmaintelligence.com/research/?file=3df1b7d57b1e63a0cbc3d585feb82dc2&download
[2] J. G. Andrews *et al.*, "What will 5G be?" *IEEE J. Sel. Areas Commun.*, vol. 32, no. 6, pp. 1065–1082, Jun. 2014.
[3] International Telecommunication Union-Radiocommunication, *IMT Vision—Framework and Overall Objectives of the Future Development of IMT for 2020 and Beyond*, document ITU-R M.2083-0, 2015.
[4] H. Viswanathan and M. Weldon, "The past, present, and future of mobile communications," *Bell Labs Tech. J.*, vol. 19, pp. 8–21, Aug. 2014.
[5] Z. Pi and F. Khan, "An introduction to millimeter-wave mobile broadband systems," *IEEE Commun. Mag.*, vol. 49, no. 6, pp. 101–107, Jun. 2011.
[6] "Understanding 5G: Perspectives on future technological advancements in mobile," GSM Assoc., London, U.K., White Paper, 2014, pp. 1–26. Accessed: May 20, 2018. [Online]. Available: https://www.gsmaintelligence.com/research/?file=141208-5g.pdf&download
[7] *The Road to 5G: Drivers, Applications, Requirements and Technical Development*, Global Mobile Suppliers Assoc., Farnham, U.K., 2015.
[8] H. T. Friis, "A note on a simple transmission formula," *Proc. IRE*, vol. 34, no. 5, pp. 254–256, May 1946.
[9] W. Roh *et al.*, "Millimeter-wave beamforming as an enabling technology for 5G cellular communications: Theoretical feasibility and prototype results," *IEEE Commun. Mag.*, vol. 52, no. 2, pp. 106–113, Feb. 2014.
[10] C. A. Ballanis, *Antenna Theory: Analysis and Design*, 4th ed. New York, NY, USA: Wiley, 2015.
[11] S. Bellofiore, C. A. Balanis, J. Foutz, and A. S. Spanias, "Smart-antenna systems for mobile communication networks. Part 1. Overview and antenna design," *IEEE Antennas Propag. Mag.*, vol. 44, no. 3, pp. 145–154, Jun. 2002.
[12] S. Bellofiore, J. Foutz, C. A. Balanis, and A. S. Spanias, "Smart-antenna system for mobile communication networks. Part 2. Beamforming and network throughput," *IEEE Antennas Propag. Mag.*, vol. 44, no. 4, pp. 106–114, Aug. 2002.
[13] M. H. Dahri, M. H. Jamaluddin, M. Khalily, M. I. Abbasi, R. Selvaraju, and M. R. Kamarudin, "Polarization diversity and adaptive beamsteering for 5G reflectarrays: A review," *IEEE Access*, vol. 6, pp. 19451–19464, 2018.
[14] W. L. Stutzman and G. A. Thiele, *Antenna Theory and Design*. Hoboken, NJ, USA: Wiley, 2012.
[15] R. C. Hansen, *Microwave Scanning Antennas*, vol. 1. New York, NY, USA: Academic, 1964.
[16] H.-S. Lui, H. T. Hui, and M. S. Leong, "A note on the mutual-coupling problems in transmitting and receiving antenna arrays," *IEEE Antennas Propag. Mag.*, vol. 51, no. 5, pp. 171–176, Oct. 2009.
[17] I. J. Gupta and A. A. Ksienski, "Effect of mutual coupling on the performance of adaptive arrays," *IEEE Trans. Antennas Propag.*, vol. AP-31, no. 5, pp. 785–791, Sep. 1983.
[18] T. Su and H. Ling, "On modeling mutual coupling in antenna arrays using the coupling matrix," *Microw. Opt. Technol. Lett.*, vol. 28, no. 4, pp. 231–237, 2001.
[19] Z. Huang, C. A. Balanis, and C. R. Birtcher, "Mutual coupling compensation in UCAs: Simulations and experiment," *IEEE Trans. Antennas Propag.*, vol. 54, no. 11, pp. 3082–3086, Nov. 2006.
[20] J. Nasir, M. H. Jamaluddin, M. R. Kamarudin, I. Ullah, Y.-C. Lo, and R. Selvaraju, "A four-element linear dielectric resonator antenna array for beamforming applications with compensation of mutual coupling," *IEEE Access*, vol. 4, pp. 6427–6437, 2016.
[21] Q. Huang, H. Zhou, J. Bao, and X. Shi, "Calibration of mutual coupling effect for adaptive arrays composed of circularly polarized microstrip antennas," *Electromagnetics*, vol. 34, no. 5, pp. 392–401, 2014.
[22] Q. Huang, H. Zhou, J. Bao, and X. Shi, "Mutual coupling calibration for microstrip antenna arrays via element pattern reconstruction method," *IEEE Antennas Wireless Propag. Lett.*, vol. 13, pp. 51–54, 2014.
[23] Y. Yu, H.-S. Lui, C. H. Niow, and H. T. Hui, "Improved DOA estimations using the receiving mutual impedances for mutual coupling compensation: An experimental study," *IEEE Trans. Wireless Commun.*, vol. 10, no. 7, pp. 2228–2233, Jul. 2011.
[24] M. H. Jamaluddin, R. Gillard, R. Sauleau, and M. A. Milon, "Perturbation technique to analyze mutual coupling in reflectarrays," *IEEE Antennas Wireless Propag. Lett.*, vol. 8, pp. 697–700, 2009.
[25] M. S. Wartak, K. L. Tsakmakidis, and O. Hess, "Introduction to metamaterials," *Phys. Canada*, vol. 67, no. 1, pp. 30–34, 2011.
[26] R. S. Kshetrimayum, "A brief intro to metamaterials," *IEEE Potentials*, vol. 23, no. 5, pp. 44–46, Dec. 2005.
[27] D. Sievenpiper, L. Zhang, R. F. J. Broas, N. G. Alexopolous, and E. Yablonovitch, "High-impedance electromagnetic surfaces with a forbidden frequency band," *IEEE Trans. Microw. Theory Techn.*, vol. 47, no. 11, pp. 2059–2074, Nov. 1999.
[28] D. Ahn, J. S. Park, C. S. Kim, J. Kim, Y. Qian, and T. Itoh, "A design of the low-pass filter using the novel microstrip defected ground structure," *IEEE Trans. Microw. Theory Techn.*, vol. 49, no. 1, pp. 86–93, Jan. 2001.
[29] D. Guha, S. Biswas, M. Biswas, J. Y. Siddiqui, and Y. M. M. Antar, "Concentric ring-shaped defected ground structures for microstrip applications," *IEEE Antennas Wireless Propag. Lett.*, vol. 5, no. 1, pp. 402–405, Dec. 2006.

[30] C.-Y. Chiu, C.-H. Cheng, R. D. Murch, and C. R. Rowell, "Reduction of mutual coupling between closely-packed antenna elements," *IEEE Trans. Antennas Propag.*, vol. 55, no. 6, pp. 1732–1738, Jun. 2007.
[31] S. Ghosh, T.-N. Tran, and T. Le-Ngoc, "Dual-layer EBG-based miniaturized multi-element antenna for MIMO systems," *IEEE Trans. Antennas Propag.*, vol. 62, no. 8, pp. 3985–3997, Aug. 2014.
[32] M. M. Bait-Suwailam, M. S. Boybay, and O. M. Ramahi, "Electromagnetic coupling reduction in high-profile monopole antennas using single-negative magnetic metamaterials for MIMO applications," *IEEE Trans. Antennas Propag.*, vol. 58, no. 9, pp. 2894–2902, Sep. 2010.
[33] S. Gupta, Z. Briqech, A. R. Sebak, and T. A. Denidni, "Mutual-coupling reduction using metasurface corrugations for 28 GHz MIMO applications," *IEEE Antennas Wireless Propag. Lett.*, vol. 16, pp. 2763–2766, 2017.
[34] Z. Qamar, L. Riaz, M. Chongcheawchamnan, S. A. Khan, and M. F. Shafique, "Slot combined complementary split ring resonators for mutual coupling suppression in microstrip phased arrays," *IET Microw., Antennas Propag.*, vol. 8, no. 15, pp. 1261–1267, 2014.
[35] M. S. Sharawi, M. U. Khan, A. B. Numan, and D. N. Aloi, "A CSRR loaded MIMO antenna system for ISM band operation," *IEEE Trans. Antennas Propag.*, vol. 61, no. 8, pp. 4265–4274, Aug. 2013.
[36] M. M. Bait-Suwailam, O. F. Siddiqui, and O. M. Ramahi, "Mutual coupling reduction between microstrip patch antennas using slotted-complementary split-ring resonators," *IEEE Antennas Wireless Propag. Lett.*, vol. 9, pp. 876–878, 2010.
[37] R. Selvaraju, M. H. Jamaluddin, M. R. Kamarudin, J. Nasir, and M. H. Dahri, "Complementary split ring resonator for isolation enhancement in 5G communication antenna array," *Prog. Electromagn. Res.*, vol. 83, pp. 217–228, Apr. 2018.
[38] F. Falcone, T. Lopetegi, J. D. Baena, R. Marques, F. Martín, and M. Sorolla, "Effective negative-ε stopband microstrip lines based on complementary split ring resonators," *IEEE Microw. Wireless Compon. Lett.*, vol. 14, no. 6, pp. 280–282, Jun. 2004.
[39] F. Falcone *et al.*, "Babinet principle applied to the design of metasurfaces and metamaterials," *Phys. Rev. Lett.*, vol. 93, no. 19, p. 197401, 2004.
[40] C. W. Hsue, Y.-W. Chang, and S.-L. Jang, "Comments on babinets principle," *Forum Electromagn. Res. Methods Appl. Technol.*, vol. 16, no. 3, pp. 1–4, 2016.
[41] J. N. Garolera, "Symmetry properties in transmission lines loaded with electrically small resonators circuit modeling and application to common-mode suppressed differential lines, microwave sensors, and spectral signature barcodes," Ph.D. dissertation, Dept. Electron. Eng., Auton. Univ. Barcelona, Bellaterra, Spain, Oct. 2014.
[42] F. J. Hsieh, C.-L. Chang, and W.-C. Wang, "Determination of effective constitutive parameters, material boundaries and properties of SRR-rod and fishnet metamaterials by Drude/Lorentz dispersion models," in *Proc. Prog. Electromagn. Res. Symp.*, Kuala Lumpur, Malaysia, Mar. 2012, pp. 036617-1–036617-11.
[43] D. R. Smith, D. C. Vier, T. Koschny, and C. M. Soukoulis, "Electromagnetic parameter retrieval from inhomogeneous metamaterials," *Phys. Rev. E, Stat. Phys. Plasmas Fluids Relat. Interdiscip. Top.*, vol. 71, no. 3, p. 036617, Mar. 2005.

RAGHURAMAN SELVARAJU was born in Gandarvakottai, India, in 1989. He received the bachelor's degree in electronics and communication engineering and the master's degree in wireless communication systems from Periyar Maniammai University, India, in 2011 and 2014, respectively. He is currently pursuing the Ph.D. degree with the Wireless Communication Centre, School of Engineering, Universiti Teknologi Malaysia. His research interests include microstrip patch antennas, dielectric resonator antennas, MIMO antennas, beamforming array antennas, mutual coupling analysis, metamaterials, and split ring resonators.

MOHD HAIZAL JAMALUDDIN received the bachelor's and master's degrees in electrical engineering from Universiti Teknologi Malaysia, Malaysia, in 2003 and 2006, respectively, and the Ph.D. degree in signal processing and telecommunications from the Université de Rennes 1, France, in 2009, with a focus on microwave communication systems and specially antennas, such as dielectric resonator and reflectarray and dielectric dome antennas. He is currently an Associate Professor with the Wireless Communication Centre, School of Electrical Engineering, Universiti Teknologi Malaysia. His research interests include dielectric resonator antennas, printed microstrip antennas, MIMO antennas, and DRA reflectarray antenna. He has published over 100 papers in reputed indexed journals and conference proceedings.

MUHAMMAD RAMLEE KAMARUDIN (M'08–SM'13) received the degree (Hons.) in electrical and telecommunication engineering from Universiti Teknologi Malaysia, Johor Bahru, Malaysia, in 2003, and the M.Sc. degree in communication engineering and the Ph.D. degree in electrical engineering from the University of Birmingham, Birmingham, U.K., in 2004 and 2007, respectively, under the supervision of Emeritus Prof. P. Hall. He was an Associate Professor with the Wireless Communication Centre, Universiti Teknologi Malaysia. He has been a Senior Lecturer with the Centre for Electronic Warfare, Information and Cyber, Cranfield Defence and Security, Cranfield University, U.K., since 2017. He has authored a book chapter of a book *Antennas and Propagation for Body-Centric Wireless Communications* and has published over 220 technical papers in journals and proceedings, including the IEEE Transaction on Antennas and Propagation, the IEEE Antennas and Wireless Propagation Letter, the *IEEE Antenna Magazine*, the IEEE Access, the *International Journal of Antennas and Propagation*, *Progress in Electromagnetic Research, Microwave and Optical Technology Letters*, and *Electronics Letters*. His research interests include antenna design for 5G, MIMO antennas, array antenna for beam-forming and beam steering, wireless on-body communications, inbody communications (implantable antenna), RF and microwave communication systems, and antenna diversity. He is a member of the IET, an Executive Member of Antenna and Propagation, Malaysia Chapter, and a member of the IEEE Antennas and Propagation Society, the IEEE Communication Society, the IEEE Microwave Theory and Techniques Society, the IEEE Electromagnetic Compatibility Society, an Associate Editor of *Electronics Letters* and *IET Microwaves, Antennas and Propagation*, and an Academic Editor of the *International Journal of Antennas and Propagation*. He holds an h-Index of 21 (SCOPUS) and over 1700 citations (SCOPUS).

JAMAL NASIR was born in Malakand Agency, Pakistan, in 1983. He received the M.Sc. degree in mobile and satellite communication from the University of Bradford, U.K., in 2007, and the Ph.D. degree in electrical engineering from Universiti Technologi Malaysia in 2017. He is currently an Assistant Professor with the Department of Electrical Engineering, COMSATS University Islamabad, Abbottabad Campus, Pakistan. His research interests include SIW-based passive components and arrays, metamaterials, smart antennas, mutual coupling analysis, MIMO antennas, dielectric resonator antennas, UWB antennas, and wearable antennas.

MUHAMMAD HASHIM DAHRI received the B.E. degree in telecommunications from the Mehran University of Engineering and Technology, Pakistan, in 2010, and the master's by research degree in electrical engineering from Universiti Tun Hussein Onn Malaysia in 2014. He is currently pursuing the Ph.D. degree with the Wireless Communication Centre, Universiti Teknologi Malaysia. He has authored over 20 research papers in various indexed journals and conference proceedings. His research interests include reflectarray antennas, planar printed antennas, and tunable materials for antenna design.